Development 128, 895-906 (2001)
Printed in Great Britain © The Company of Biologists Limited 2001
DEV1632

A role for the EphA family in the topographic targeting of vomeronasal axons

Bernd Knöll[1,*], Konstantinos Zarbalis[2,3,*], Wolfgang Wurst[2,3,§] and Uwe Drescher[1,‡,§]

[1]Department of Physical Biology, Max-Planck-Institute for Developmental Biology, Spemannstrasse 35 / I, 72076 Tübingen, Germany
[2]Clinical Neurogenetics, Max-Planck-Institute of Psychiatry, Kraepelinstr. 2, 80804 Munich, Germany
[3]GSF-Research Centre, Institute for Mammalian Genetics, Ingolstaedter Landstr. 1, 85764 Neuherberg, Germany
*These authors contributed equally to this work
‡Present address: MRC Centre for Developmental Neurobiology, King's College London, 4th Floor, New Hunt's House, Guy's Campus, London SE1 1UL, UK
§Authors for correspondence (e-mail: uwe.drescher@kcl.ac.uk and wurst@mpipsykl.mpg.de)

Accepted 18 December 2000; published on WWW 26 February 2001

SUMMARY

We have investigated the role of the Eph family of receptor tyrosine kinases and their ligands in the establishment of the vomeronasal projection in the mouse. Our data show intriguing differential expression patterns of ephrin-A5 on vomeronasal axons and of EphA6 in the accessory olfactory bulb (AOB), such that axons with high ligand concentration project onto regions of the AOB with high receptor concentration and vice versa. These data suggest a mechanism for development of this projection that is the opposite of the repellent interaction between Eph receptors and ligands observed in other systems. In support of this idea, when given the choice of whether to grow on lanes containing EphA-F_c/laminin or F_c/laminin protein (in the stripe assay), vomeronasal axons prefer to grow on EphA-F_c/laminin. Analysis of ephrin-A5 mutant mice revealed a disturbance of the topographic targeting of vomeronasal axons to the AOB. In summary, these data, which are derived from in vitro and in vivo experiments, indicate an important role of the EphA family in setting up the vomeronasal projection.

Key words: Eph, Topographic projection, Mouse, Ephrin, Vomeronasal, Mouse

INTRODUCTION

A central process during development of the nervous system is the guidance of axons from their site of origin to their target area. A large number of molecules have been shown to be involved in this process, such as the netrins and their receptors (Dcc and Unc5), the semaphorins and the neuropilin and plexin receptors, the Slits and Robos, as well as the ephrins, which interact with receptor tyrosine kinases of the Eph family (Müller, 1999; Tessier-Lavigne and Goodman, 1996).

This latter family comprises 14 different receptors and eight ligands so far, all of which are widely expressed in the central and peripheral nervous systems during development and in adult. Individual members of the Eph family have been implicated in axon guidance as well as in a number of other (possibly related) processes, such as cell migration, boundary formation through restricting cell intermingling, axonal pathfinding, layer-specific arborisations in the target area and angiogenesis (for reviews, see Flanagan and Vanderhaeghen, 1998; Frisen et al., 1999; Holder and Klein, 1999; O'Leary and Wilkinson, 1999; Wilkinson, 2000).

At present, an overwhelming number of reports indicate that the Eph family exerts its function by a repellent mechanism, although there are some reports of an adhesive or permissive function of Eph receptors and ligands (Daniel et al., 1996; Davy et al., 2000; Davy et al., 1999; Holash et al., 1997; Holmberg et al., 2000; Huai and Drescher, 2001; Huynh-Do et al., 1999; Pandey et al., 1995; Stein et al., 1998).

The Eph family can be subdivided into two classes: EphA receptors interact with glycosylphosphatidylinositol (GPI)-anchored ephrin-A ligands and the EphB receptors interact with ephrin-B ligands, which are transmembrane anchored. This subdivision is strictly followed, the only exception being the EphA4 receptor, which interacts with both ephrin-A and ephrin-B molecules.

Within both families, bi-directional signalling has been observed, such that interaction of the respective axons or cells leads to an activation of specific signalling pathways in the 'receptor'-expressing cell as well as in the 'ligand' expressing cell (Brückner et al., 1997; Davy et al., 2000; Davy et al., 1999; Henkemeyer et al., 1996; Holland et al., 1996; Huai and Drescher, 2001). This has been shown, for example, in case of the anterior commissure, where axons expressing ephrin-B ligands are guided by Eph receptors located in the immediate vicinity of migrating axons (Brückner and Klein, 1998; Holland et al., 1998), as well as in the processes leading to the segmental patterning in the hindbrain (Mellitzer et al., 1999; Xu et al., 1999). For the EphA family, such a role has been observed so far for fibroblast cells, where binding of EphA receptors to ephrin-A-expressing cells leads to an β1-integrin-dependent upregulation of the adhesiveness of these cells (Davy et al., 2000; Davy et al., 1999; Huai and Drescher, 2001).

Members of the Eph family are involved in the development

of topographically organised projections such as the retinotectal projection (for reviews, see Drescher et al., 1997; Flanagan and Vanderhaeghen, 1998; O'Leary et al., 1999). Recent advances in the molecular and topographical study of the vomeronasal organ (VNO) in mammals have offered a valuable experimental system in which the role of the EphA family in establishing functional sensory connections can be further characterised. The VNO is a distinct and bilaterally symmetric structure of the ventral nasal septum of terrestrial vertebrates that is primarily responsible for the detection of pheromones (for reviews, see Bargmann, 1999; Buck, 2000; Dulac, 2000; Halpern, 1987; Keverne, 1999).

VNO axons are sent out from the vomeronasal epithelium very early in development, i.e. from embryonic day (E) 11 onwards (Hinds, 1968). Later, the axons travel along the septum, cross the cribiform plate and project fasciculated along the medial surface of the olfactory bulb. The VNO projections then bypass the main olfactory bulb to enter the accessory olfactory bulb (AOB), located dorsal to the main olfactory bulb, from its medioposterior end. The AOB is detectable as a morphologically distinct structure from about E15 onwards. Ingrowth of vomeronasal axons into the AOB occurs prenatally. At postnatal day (P) 1, glomeruli have begun to form, and the different layers of the AOB (see Fig. 1) can be easily recognised. As judged from the localisation of transneuronal markers, functional synapses are not formed until the first postnatal days, i.e. the vomeronasal system does not become active until after birth (Horowitz et al., 1999; Keverne, 1999).

The AOB, in turn, projects to specific nuclei of the medial amygdala (see, for example, von Campenhausen and Mori, 2000). Pheromone signals ultimately result in the activation of centres of the preoptic and ventromedial hypothalamus that are involved in reproductive and aggressive behaviours. The vomeronasal system provides a unique experimental system with which to uncover the basic mechanisms that control the development of neural networks involved in genetically pre-programmed behaviours.

Two independent families of vomeronasal receptor genes have been characterised, the V1Rs and V2Rs, that encode seven-transmembrane domain proteins thought to represent the mammalian pheromone receptors (Dulac and Axel, 1995; Herrada and Dulac, 1997; Matsunami and Buck, 1997; Ryba and Tirindelli, 1997). The V1R and the V2R receptor families are expressed by two spatially segregated populations of VNO sensory neurones, such that neurones lining the apical half of the VNO neuroepithelium co-express V1Rs and the G-protein α subunit, $G_{\alpha i2}$, whereas neurones of the basal half of the VNO are both V2R and $G_{o\alpha}$ positive (reviewed by Dulac, 2000). Immunocytochemistry suggest that fibres reaching the AOB are likely to stay segregated according to their origin (from either the apical or basal sides of the VNO), with $G_{\alpha o}$-positive fibres projecting to the posterior half of the AOB and $G_{\alpha i2}$-positive fibres reaching the anterior portion of the AOB (Berghard and Buck, 1996; Berghard et al., 1996; Ichikawa et al., 1994; Imamura et al., 1985; Jia and Halpern, 1996; Krieger et al., 1999; von Campenhausen et al., 1997).

In order to gain more direct access into the sensory map of pheromone receptor activation in the AOB, the genes for V1Rs have been genetically modified in order to allow co-translation of the endogenous receptor along with a tau-*lacZ* or tau-GFP reporter protein (Belluscio et al., 1999; Rodriguez et al., 1999). In these mice, it is possible to directly visualise the pattern of projections of subpopulations of VNO neurones expressing a given pheromone receptor in the brain. These experiments have revealed the existence of a complex, yet spatially conserved, topographic map of VNO receptor projections, according to which the AOB is organised into large domains of sensory projections. Each projection domain comprises multiple glomeruli and receives input from several receptor populations of VNO neurones.

How is the vomeronasal map established during development? Analysis of AOBs of 6- to 8-week old mice from lines in which the gene for a V1R pheromone receptor is deleted shows that axons are unable to reach their target and widely 'wander' throughout the AOB glomerular layer

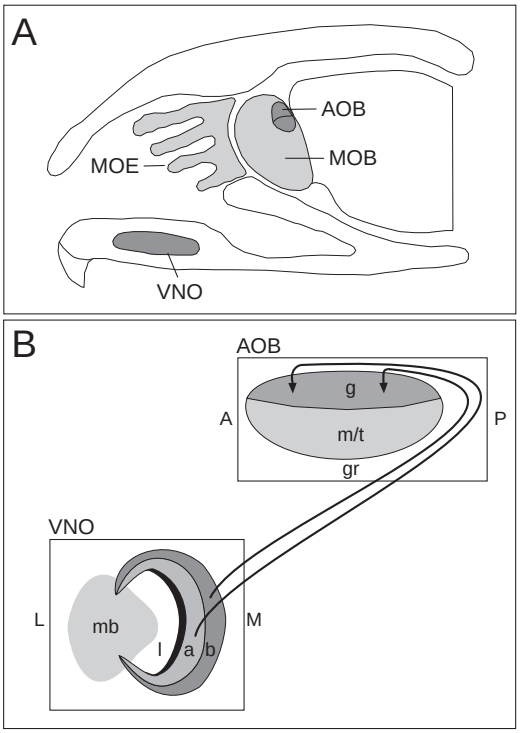

Fig. 1. Anatomy of the olfactory system. (A) The main olfactory system and the vomeronasal system. The main olfactory epithelium (MOE) is located in the dorsal aspect of the nasal cavity, from where axons grow through the cribiform plate and project to the main olfactory bulb (MOB), which represents an evagination of the telencephalon. The vomeronasal system consists of the vomeronasal organ (VNO) in the ventral aspect of the nasal cavity and the target area of vomeronasal axons, the accessory olfactory bulb (AOB), positioned dorsoposteriorly on top of the MOB. (B) Zone-to-zone projection from the VNO to the AOB. Axons from the apical part of the VNO (a) project to the anterior part of the AOB, and axons from the basal part of the VNO (b) connect to the posterior part of the AOB. Within the AOB, the VNO axons synapse with dendrites of mitral/tufted cells (m/t) in the glomerular layer (g). Within the glomerular layer, ingrowing vomeronasal axons form superficially the vomeronasal nerve layer. Dorsal is towards the top, ventral towards the bottom. The non-sensory epithelium close to the lumen is shown in black. a, apical; A, anterior; b, basal; g, glomerular layer; gr, granular cell layer; l, lumen; L, lateral; M, medial; mb, mushroom body; m/t, mitral/tufted cell layer; P, posterior.

(Belluscio et al., 1999; Rodriguez et al., 1999). The inability of VNO neurones that lack V1R expression to reach the appropriate domain in the AOB suggests that the receptor molecule may play a role in guiding sensory axons to the right target in the brain. The role of the receptor might be simply permissive and linked to the pheromone receptor sensory activity, or, as it has been more clearly demonstrated in the main olfactory system by genetic swap of receptor coding sequences (Wang et al., 1998), it may directly play a role as an instructive guidance receptor.

We have analysed the expression pattern of the entire A-subclass of Eph receptors and ligands in the vomeronasal system of the mouse during various stages of development and in adult mice. Our data show intriguing differential expression patterns of in particular ephrin-A5 on vomeronasal axons and of EphA6 in the AOB. Results from in vitro and in vivo experiments provide evidence that the EphA family plays an instructive role in establishing the vomeronasal projection. We also show that ephrin-As have a function as axon guidance receptors.

MATERIALS AND METHODS

Animals

C57BL/6 mice were anaesthetised with diethylether prior to cervical dislocation at the indicated gestational and postnatal stages. Gestation was dated day 0.5 on the day a vaginal plug was visible. For all experiments performed, tissues were embedded without prior fixation in OCT compound (Tissue-Tek; Miles, Elkhart, IN) and frozen on dry ice. Tissues were sectioned at 20 μm for alkaline phosphatase (AP) staining, 16 μm for immunohistochemistry and 14 μm for mRNA in situ hybridisation.

Sections were collected on superfrost slides and air-dried at room temperature overnight for AP staining, for 2 hours for immunohistochemistry and for 20 minutes for in situ hybridisation.

Staining of sections with AP fusion proteins

For the construction and expression of EphA3-AP, ephrin-A5-AP and AP fusion proteins, see Ciossek et al. (Ciossek et al., 1998) and Flanagan and Leder (Flanagan and Leder, 1990). Sections were rehydrated for 10 minutes in HBHA (0.5 mg/ml BSA, 0.1% NaN_3, 20 mM Hepes pH 7.0 in HanksA) and incubated with 7 nM of the indicated AP fusion protein for 2 hours. The sections were rinsed four times in HBS (20 mM Hepes pH 7.0, 150 mM NaCl), fixed for 90 seconds in 60% acetone, 3.7% formaldehyde, 20 mM Hepes pH 7.0 and washed six times in HBS. Endogenous alkaline phosphatases were inactivated for 1 hour at 65°C, counterstained with DAPI and incubated for 10 minutes in AP buffer (0.1 M Tris/HCl pH 9.5, 0.1 M NaCl, 5 mM $MgCl_2$ in H_2O). The sections were rinsed for another 10 minutes in AP buffer and 10 mM homoarginine and finally incubated in the same buffer with 3.5 μl 4-nitroblue tetrazolium chloride (NBT) and 4.5 μl 5-bromo-4-chloro-3-indolyl-phosphate (BCIP; both from Roche) per ml.

AP staining on VNO explants

Explants grown for 2 days on laminin or fibronectin were washed once at room temperature with PBS and incubated for 1.5 hours in 7 nM of the indicated AP fusion proteins. Explants were washed six times with HBHA, fixed for 30 seconds and washed twice in HBS. Endogenous alkaline phosphatases were inactivated for 15 minutes at 65°C and explants were rinsed for 10 minutes in AP-buffer and developed in AP-buffer with NBT/BCIP. The reaction was stopped with PBS after the desired colour intensity had been reached.

In situ hybridisation

mRNA in situ hybridisation was performed as described previously (Schaeren-Wiemers and Gerfin-Moser, 1993). The anti-DIG antibody was applied diluted 1:7500 overnight at 4°C. Digoxigenin-labelled cRNA probes were generated by using full-length clones and restriction sites within for ephrin-A5 (nucleotides 400-728 with *Eco*RI; A. Flenniken), EphA3 (nucleotides 2812-3197 with *Eco*RV; E. Pasquale), EphA4 (nucleotides 3194-4241 with *Nco*I; A. Flenniken) and EphA7 (nucleotides 1222-1847 with *Stu*I; T. Ciossek). For the other cRNA probes, DNA fragments were generated by RT-PCR (cDNA cycle Kit; Invitrogen) from poly-A^+-RNA (micro fast track 2.0; Invitrogen) isolated from mouse E17.5 hippocampus (ephrin-A4) or P1 total brain (ephrin-A2, ephrin-A3, ephA5 and ephA6). The ephA2 fragment was generated from embryonic stem cell cDNA. All DNA fragments were cloned in pBluescriptKS vector (Stratagene). Sequence specific antisense and sense primers (flanked with *Eco*RI and *Bam*HI sites) were used to amplify DNA fragments spanning nucleotides 748-978 for ephrin-A2, 2165-2485 for ephrin-A3, 326-789 for ephrin-A4, 3070-3450 for EphA2, 1401-1707 for EphA5 and 3071-3571 for EphA6. The identity of the fragments was verified by sequencing.

VNO explants

VNOs from E14.5 to P1 mice were dissected in neurobasal medium with B27 supplement containing 0.5 μg/ml fungizone, 5 μg/ml gentamycin and methyl-cellulose (diluted 1:3; all from Gibco). The sensory epithelium was cut into pieces of about 1 mm^3. Explants were cultured on 15 mm acid-cleaned glass-coverslips coated with poly-L-lysine (Sigma; 1 mg/ml overnight at 37°C in borate buffer, pH 8.5) and laminin (Becton Dickinson; 3-5 μg/ml in PBS for 3 hours at 37°C) in the preparation medium and kept in an incubator with a humid atmosphere containing 4% CO_2 at 37°C.

Generation of *ephrin-A5*$^{-/-}$ mice and analysis of VN12-tau-*lacZ*, *ephrin-A5*$^{-/-}$ mice

A detailed description of the generation of *ephrin-A5*$^{-/-}$ (*Efna5*$^{-/-}$) mice will be published elsewhere (K. Z. and W. W.). The genetic background of both *ephrin-A5*$^{-/-}$ and VN12-tau-*lacZ* mice is 129SV × C57BL/6. The F_1 generation from *ephrin-A5*$^{-/-}$ and VN12-tau-*lacZ*$^{+/+}$ mice was crossed to each other and the F_2 generation was genotyped by PCR for ephrin-A5 using the primers 5′-CAAG-GAGACATCTGTAACACAGAGTCC-3′, 5′-CACATTGATGTCTG-TATCAATGACTACC-3′ and 5′-ATCGATCCGTCCTGTAAGTCT-GC-3′ with 35 cycles (95°C, 30 seconds; 55°C, 30 seconds; 72°C, 30 seconds). This resulted in fragments of 402 bp for wild type and of 670 bp for the mutated allele. The presence of *lacZ* was analysed using the primers 5′-GGTGGCGCTGGATGGTAA-3′ and 5′-CGCCATT-TGACCACTACC-3′ with the same protocol as used for ephrin-A5 genotyping, here leading to a fragment of 600 bp. This protocol did not allow us to discriminate between mice with two or only one allele of *lacZ*. Mice positive for *lacZ* and heterozygous for ephrin-A5 were used for repeated rounds of subsequent breeding. Littermates of such crosses were the basis for the analysis of the projection pattern of VNO axons.

Stripe assay

The stripe assay has been performed as described in Hornberger et al. (Hornberger et al., 1999). The protein concentrations used were 8 μg/ml clustered EphA7-F_c for the first stripe and 3 μg/ml clustered F_c for the second stripe, in the controls 8 μg/ml clustered F_c for the first stripe and 3 μg/ml clustered F_c for the second stripe. Laminin concentrations used were 5 μg/ml. The same medium as for the VNO explants has been used. It is likely that – based on binding affinities (Gale et al., 1996) – the use of an EphA6-F_c construct leads to a similar behaviour of vomeronasal axons in the stripe assay as the EphA7-F_c construct used here.

RESULTS

Expression of the EphA family in the developing vomeronasal system

A high promiscuity has been shown in the interaction of Eph receptors and ligands, such that within a subfamily each receptor can interact with each ligand and vice versa. As a result, the functional characterisation of the Eph family in a specific system requires an understanding of the expression pattern of all members of the Eph subclass. In order to establish whether members of the EphA family might be involved in the formation of the VNO-AOB projection, we have studied the expression patterns of all relevant members of the EphA family both at the protein and the mRNA levels. We have included in this analysis the ligands ephrin-A2 to ephrin-A5 and the receptors EphA2 to EphA7, but have excluded ephrin-A1 and EphA1, as both of these are known not to be expressed in the nervous system (Zhou, 1998). We have also omitted EphA8, as it is only expressed in the superior and inferior colliculi (Park et al., 1997).

Early embryonic stages E12.5

We started the analysis at E12.5, shortly after VNO axons are sent out from the vomeronasal epithelium. In initial experiments, shown in Fig. 2, we analysed cryostat sections with fusion proteins of alkaline phosphatase (AP) linked to either the extracellular part of EphA receptors or to ephrin-A ligands (Cheng and Flanagan, 1994). Owing to the extended

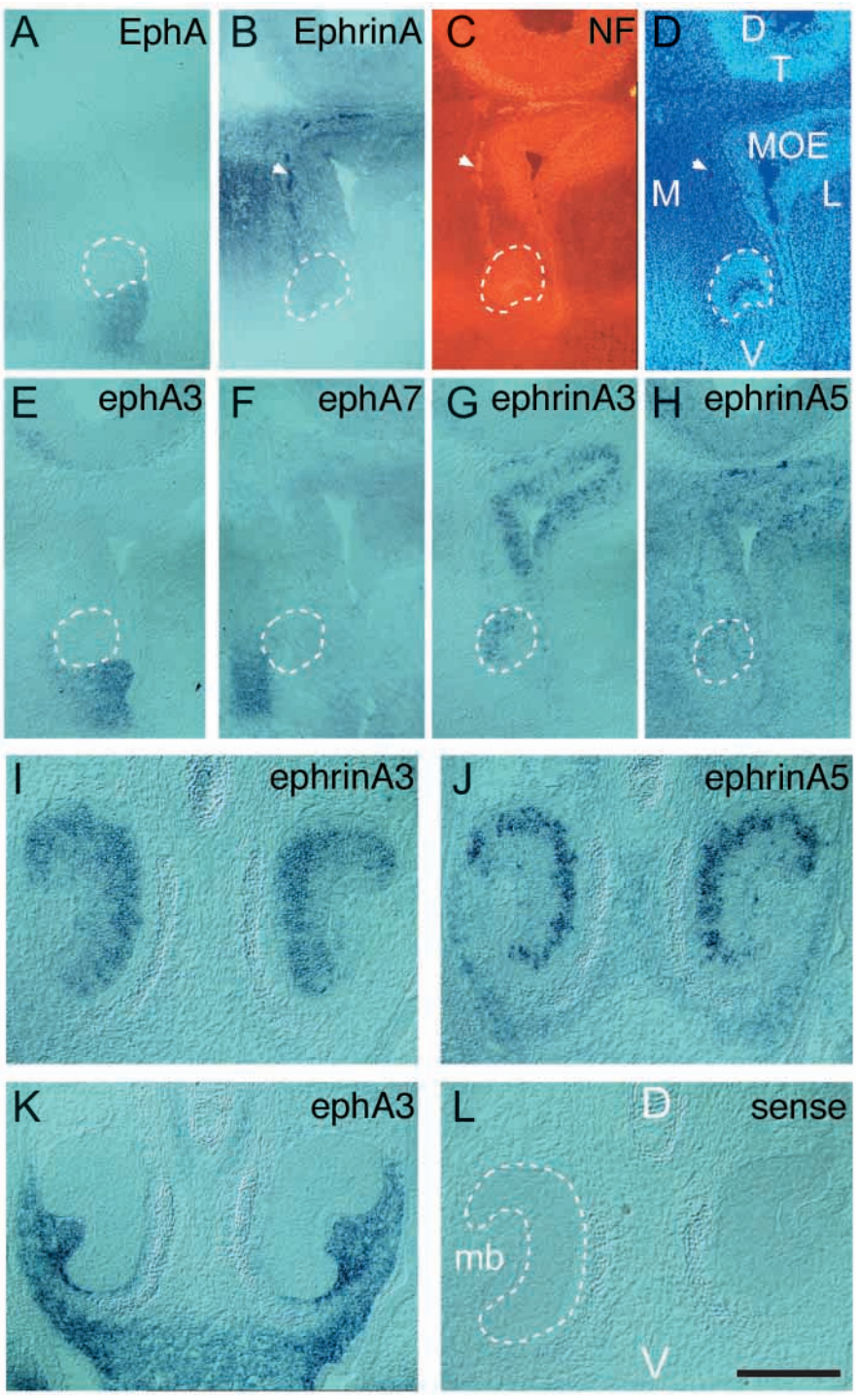

Fig. 2. Expression pattern of members of the Eph family in the developing vomeronasal organ at E 12.5 and E15.5. (A) The protein expression pattern of EphA receptors was investigated in coronal sections by staining with ephrin-A5-AP, which binds to all EphA receptors (→ EphA). The VNO, labelled by a broken line, does not express EphA receptors. (B) The protein expression pattern of ephrin-A ligands is detected by staining sections with EphA3-AP, which binds all ephrin-As (→ ephrin-A). (C,D) Adjacent sections to A,B stained with a neurofilament-specific antibody to locate axonal fibres (C), and with DAPI, to highlight the morphology of the developing VNO (D). Arrowheads in B-D indicate the vomeronasal nerve emanating from the VNO and projecting dorsally towards the telencephalon (T). (E-H) mRNA expression analysis of EphA family members. The expression of EphA3 (E), EphA7 (F), ephrin-A3 (G), ephrin-A5 (H). In addition to their expression in the VNO (broken line), ephrin-A3 is found also strongly expressed in the main olfactory epithelium (MOE), and ephrin-A5 in the surrounding mesenchyme. EphA3 expression is found ventrolaterally to the VNO, whereas EphA7 is expressed in a domain in-between the VNOs. The expression of all other EphA family members was also investigated, but none of them was found to be expressed in this region at that developmental time. (I-L) mRNA expression patterns of EphA family members in the vomeronasal system at E15.5. Expression in the VNO of ephrin-A3 (I), ephrin-A5 (J) and EphA3 (K). Although ephrin-A3 is uniformly expressed, ephrin-A5 shows a more diffuse or patchy expression pattern. (L) In situ hybridisation using an ephrin-A3 sense probe. Scale bar: 100 μm. D, dorsal; L, lateral; M, medial; V, ventral; mb, mushroom body.

promiscuity in receptor-ligand interaction within the EphA family, ephrin-A5-AP and EphA3-AP were used to detect the expression patterns of (respectively) the entire EphA receptor class (Fig. 2A) and all ephrin-A ligands (Fig. 2B). Although the results of such experiments generally have to be interpreted with some caution (Sobieszczuk and Wilkinson, 1999), they provide a rather good overview of the general distribution of Eph ligands and receptors.

This analysis showed that, at E12.5, there was strong expression of ephrins along the vomeronasal nerve containing glial cells, axons and migrating luteinizing hormone releasing hormone (LHRH) cells (Fig. 2B, arrowhead). An adjacent section was stained with an anti-neurofilament antibody (Grant et al., 1995) to confirm this staining pattern as that of the vomeronasal nerve (Fig. 2C; arrow). In addition, using DAPI staining (Fig. 2D; the VNO is marked by a broken line), the same region appeared to be free of cell bodies.

Using mRNA in situ hybridisation we were able to detect expression of ephrin-A3 and ephrin-A5 in the VNO (Fig. 2G,H). The other ligands investigated (ephrin-A2, ephrin-A4) showed no specific expression in this region. These data indicate that the ligands ephrin-A3 and ephrin-A5 are expressed on the earliest axons of the vomeronasal nerve. Additional expression of ephrin-A3 and ephrin-A5 is seen in the main olfactory epithelium (MOE), and ephrin-A5 expression is also present in the mesenchyme surrounding the VNO and the MOE (Fig. 2H), which is similar to the EphA3-AP staining pattern (Fig. 2B).

By staining with ephrin-A5-AP, we detected EphA receptor expression in a ventrolateral position adjacent to the VNO, but neither in the organ itself nor on the vomeronasal nerve (Fig. 2A). This fits in with mRNA in situ hybridisation analyses, which showed that none of the six EphA receptors investigated was expressed in the VNO. However, EphA3 mRNA is localised ventral to the VNO (Fig. 2E) and EphA7 mRNA is found medially in a broad stripe between the two VNOs (Fig. 2F). Fig. 2L shows a control hybridisation with an ephrin-A3 sense probe.

Expression at E15.5

At E15.5, vomeronasal axons have reached the accessory olfactory bulb and synaptogenesis with AOB mitral cells begins. The in situ hybridisation analysis showed that, as at E12.5, only ephrin-A3 and ephrin-A5 are expressed in the VNO (Fig. 2I,J). However, it is now apparent that both ligands are differentially expressed in the sensory epithelium: there is uniform ephrin-A3 expression (Fig. 2I) but patchy distribution of ephrin-A5 (Fig. 2J), with clusters of cells expressing different levels of ephrin-A5. Low, but specific expression of ephrin-A5 is seen also in the mesenchyme surrounding the VNO (Fig. 2J). The EphA3 receptor (Fig. 2K) is co-expressed in a ventrolateral position with ephrin-A5, albeit at a much higher level than ephrin-A5 (arrows). There is additional strong expression of EphA3 in the so-called mushroom body (mb) on the lateral side of the vomeronasal lumen. The EphA7 receptor expression depicted at E12.5 is no longer detectable at E15.5.

Expression at P1 in the VNO

At around P1, glomeruli containing functional synapses are distinguishable (Horowitz et al., 1999). Staining sections with AP-fusion proteins showed that ephrin-A ligands are expressed throughout the VNO (Fig. 3A) with strongest staining at the medial margin of the sensory epithelium (arrowheads), where VNO axons converge and project dorsally toward the AOB.

EphA receptors are expressed in some regions of the VNO reciprocally to the ligands, e.g. at the border between sensory and non-sensory epithelium (Fig. 3B, arrowheads). Staining was found also in the mushroom body of the VNO (Fig. 3B).

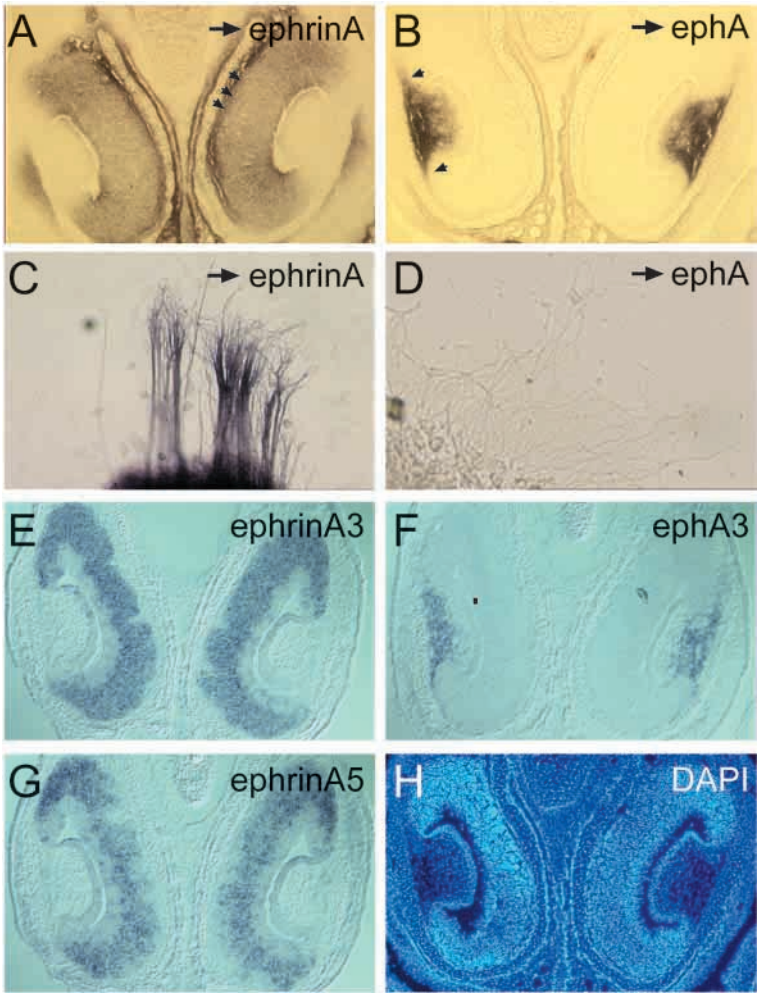

Fig. 3. Expression pattern of EphA family members at P1 in the VNO. (A) Protein expression of ephrin-A ligands in the VNO as detected by staining with EphA3-AP, which binds all ephrin-A ligands. (B) Protein expression pattern of EphA receptors detected by ephrin-A5-AP staining. (C,D) Staining of axons from vomeronasal explants with EphA3-AP for detection of ephrin-A ligand expression (C), and with ephrin-A5-AP to detect the expression of EphA receptors (D). This staining indicates that ephrin-A ligands, but not EphA receptors, are expressed on vomeronasal axons at P1. (E-G) mRNA expression patterns of ephrin-A3 (E), EphA3 (F) and ephrin-A5 (G). (A) and (B) are adjacent sections, (H) represents the DAPI picture of B, to highlight the structure of the VNO (see Fig. 1). (A,B) and (E-H) show coronal sections of the VNO.

To further demonstrate the expression of ephrin-A ligands on VNO axons, we prepared explant cultures of the VNO. Outgrowing axons were stained with AP-fusion proteins after 2 days in culture. We found strong expression of ephrin-A ligands, while staining for EphA receptors was negative (Fig. 3C,D). These results fit well with data obtained from mRNA in situ hybridisations, suggesting that the axonal ligand staining is due to the expression of ephrin-A3 and ephrin-A5 (Fig. 3E,G). Furthermore, staining of receptors in the mushroom body is due to EphA3 expression (Fig. 3F).

Expression at P1 in the AOB

We then investigated the expression of EphA-family members in the developing AOB, the site of axonal projections from the VNO sensory neurones. Fig. 4A shows the expression of ephrin-A ligands by staining coronal sections with EphA3-AP. Staining is apparent throughout the superficial nerve layer and glomerular layer, whereas EphA receptors can be detected in the glomerular and mitral/tufted cell layers of the AOB, thus partially overlapping with expression of A-ephrins (compare Fig. 4A with 4B, which are adjacent sections stained with EphA3-AP and ephrin-A5-AP, respectively). EphA receptors are also expressed in the granular cell layer.

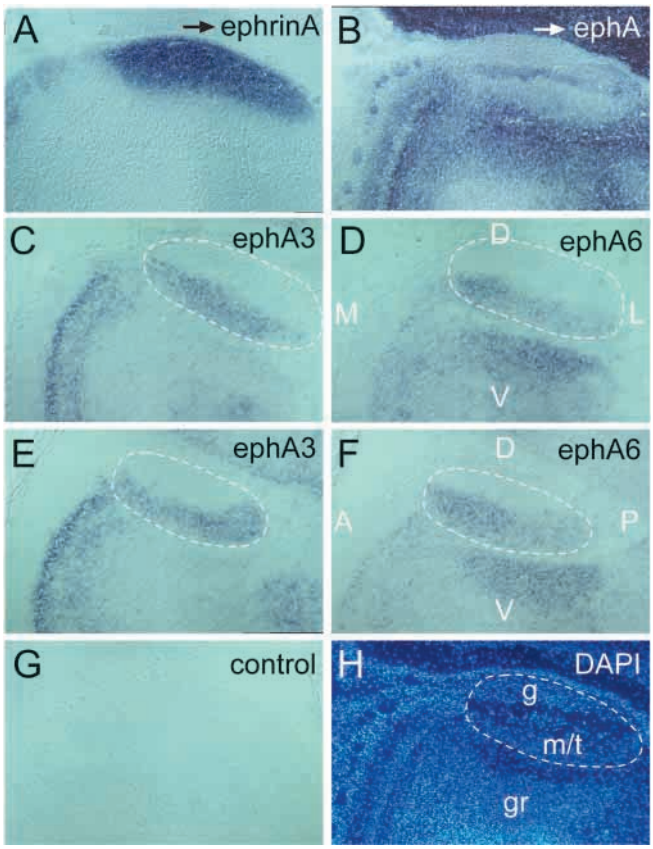

Fig. 4. Expression pattern of EphA family members at P1 in the AOB. (A) Protein expression of ephrin-A ligands detected by EphA3-AP (→ ephrin-A). (B) Protein expression pattern of EphA receptors detected by ephrin-A5-AP (→ EphA). (C,E) Sagittal (E) and coronal (C) sections probed with an EphA3-specific antisense mRNA. (D,F) Sagittal (F) and coronal (D) sections analysed using an EphA6-specific probe. (G) Control staining using an ephrin-A3 sense RNA probe. (H) represents the section shown in B using a DAPI filter to highlight the structural features of this organ (compare with Fig. 1B). The AOB in (C-F,H) is circled with a broken white line. All other EphA family members are not expressed in the vomeronasal system at that time. A,B,H are adjacent sections. A, anterior; D, dorsal; g, glomerular layer; gr, granular cell layer; L, lateral; M, medial; m/t, mitral/tufted cell layer; P, posterior; V, ventral.

At P1, there is a clear mRNA expression of ephrin-A3 and a rather weak expression of ephrin-A5 in the mitral/tufted cell layer of the AOB (data not shown). Thus, the EphA3-AP staining seen in Fig. 4A results from the expression of A-ephrins on both VNO axons and mitral/tufted cells.

Similarly, the mRNA expression patterns of EphA receptors (Fig. 4C-F) correlate with the protein expression data. EphA3 mRNA is detected uniformly in the mitral/tufted cell layer, from where dendrites are send out dorsally into the glomerular layer. Furthermore, as seen at E15.5 (data not shown), there is an asymmetric expression of EphA6 in the mitral/tufted cell layer – higher in the anterior/medial part of the AOB than in the posterior/lateral part (Fig. 4D,F). In contrast, in the granular cell layer the EphA6 receptor shows an inverse expression pattern, which is higher in the posterior/lateral part than the anterior/medial part (Fig. 4D,F).

Finally, expression analysis of the EphA family in the vomeronasal system at P12 showed a similar pattern of ephrin-A5 and ephrin-A3 (Figs 2I-J, 3E,G; see also below). In contrast, EphA3 is expressed at a lower level than at P1 in the VNO; also, the differential expression of ephA6 in the AOB is no longer as pronounced as at earlier time points (data not shown).

The expression pattern of ephrin-A5 parallels the compartmentalisation within the VNO

The differential localisation of ephrin-A5 mRNA contrasts with the uniform distribution of ephrin-A3 transcripts in the VNO at P1 (Fig. 5A-D) and 4 weeks after birth (Fig. 5E-H). A comparison of these expression patterns with those of $G_{\alpha i2}$ and $G_{\alpha o}$, which represent markers for apical and basal VNO, respectively, indicates that at both P1 and in the adult, ephrin-A5 expression correlates with that of $G_{\alpha i2}$, i.e. with a bias towards the apical part of the VNO at P1 (Fig. 5B,C), and a confinement mostly to this part four weeks later (Fig. 5F,G). Thus, the developmentally controlled segregation of $G_{\alpha i2}$ (V1R) and $G_{\alpha o}$ (V2R)-expressing cells into two distinct compartments of the VNO parallels the increasing restriction of ephrin-A5 expression to one of these zones.

Analysis of the zonal projection pattern of vomeronasal axons in ephrin-A5 mutant mice

Based on the differential expression pattern of ephrin-A5 in the developing VNO neuroepithelium, we addressed its potential function in the development of the vomeronasal projections. *ephrin-A5*$^{-/-}$ mice were analysed in the background of VN12-tau-*lacZ* mice (Figs 6, 7). The generation of *ephrin-A5*$^{-/-}$ mice will be described elsewhere (see Materials and Methods). In VN12-tau-*lacZ* mice (Belluscio et al., 1999), the genomic locus of a vomeronasal receptor, VN12, has been modified by homologous recombination (Callahan and Thomas, 1994; Mombaerts et al., 1996) in order to generate a bi-cistronic mRNA that leads to the simultaneous expression of both the VN12 receptor and tau-β-galactosidase (Belluscio et al., 1999). The

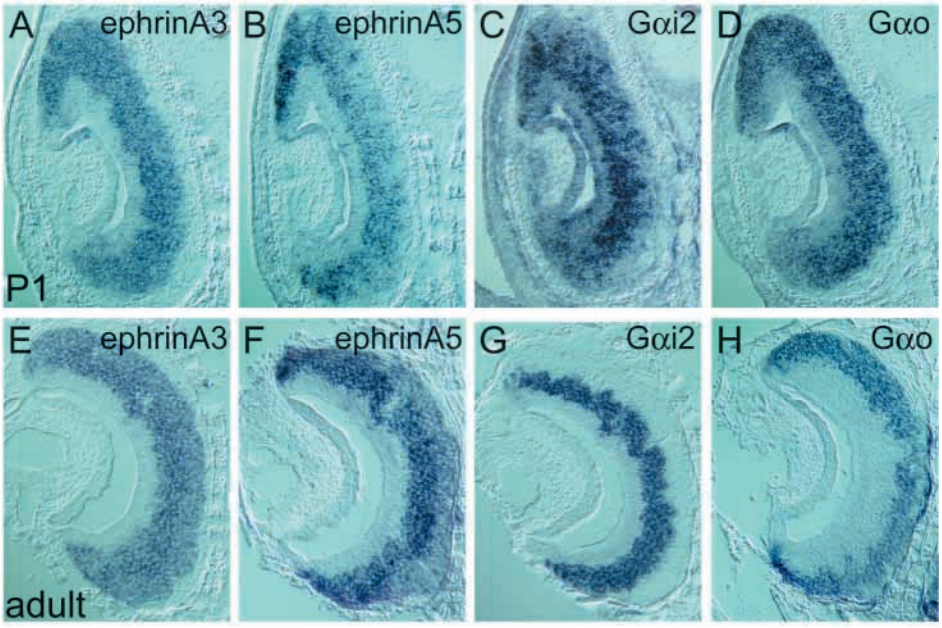

Fig. 5. Analysis of the expression pattern of ephrin-A3 and ephrin-A5 during development of the VNO-AOB projection. (A-D) Expression pattern at P1 of ephrin-A3 (A), ephrin-A5 (B), $G_{\alpha i2}$ (C), $G_{\alpha o}$ (D). At this developmental time point, cells that express ephrin-A3 or $G_{\alpha o}$ are fairly randomly distributed between the apical and basal part of the VNO. However, there appears to be a bias towards the apical domain for both $G_{\alpha i2}$ and ephrin-A5. (E-H) Expression pattern in the adult animal (>4 weeks), with ephrin-A3 (E), ephrin-A5 (F), $G_{\alpha i2}$ (G) and $G_{\alpha o}$ (H), There is a clear separation of $G_{\alpha i2}$- and $G_{\alpha o}$-expressing cells. The expression domain of ephrin-A5 is also largely confined to the apical VNO, but there appears to be some residual staining in the basal VNO. In contrast, ephrin-A3 appears uniformly expressed.

establishment of these crosses makes it possible to analyse directly, and with high resolution, the projections of VN12-expressing axons in *ephrin-A5*$^{-/-}$ mice.

Parasagittal sections of the AOB from VN12-tau-*lacZ*$^{+}$;*ephrin-A5*$^{+/+}$ and VN12-tau-*lacZ*$^{+}$;*ephrin-A5*$^{-/-}$ 6-8 weeks old mice were stained for *lacZ* expression. A neutral red staining was added, in order to visualise the overall structure of the AOB. In total, we analysed 14 VN12-tau-*lacZ*$^{+}$;ephrin-A5$^{+/+}$ and 14 VN12-tau-*lacZ*$^{+}$;*ephrin-A5*$^{-/-}$ mice.

In agreement with the data from Belluscio et al. (Belluscio et al., 1999), β-galactosidase-positive axons from VN12-tau-*lacZ*$^{+}$;*ephrin-A5*$^{+/+}$ mice projected to the anterior AOB, where they formed a complex pattern of glomeruli (Fig. 6, top row, white arrows; *n*=13/14). In only one case we observed a partial

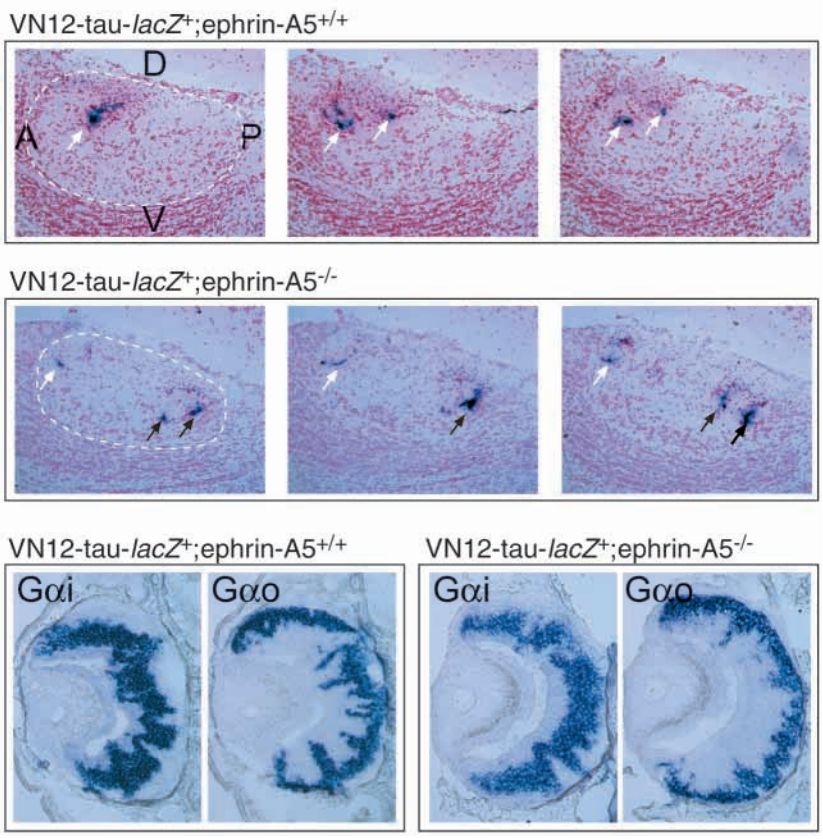

Fig. 6. Analysis of the projection patterns of VN12 receptor-expressing vomeronasal axons in wild-type and *ephrin-A5*$^{-/-}$ mice. Parasagittal sections of AOBs of littermates derived from VN12-tau-*lacZ* mice heterozygous for ephrin-A5 (VN12-tau-*lacZ*$^{+}$;*ephrin-A5*$^{+/-}$) were stained for tau-*lacZ* to localise VN12 expressing axons. In some pictures, the AOB is circled with a broken white line. To visualise the morphology of the AOB, sections were counterstained with neutral red. The top row shows the analysis of VN12-tau-*lacZ*$^{+}$;*ephrin-A5*$^{+/+}$ (wild-type) mice, the middle row the analysis of VN12-tau-*lacZ*$^{+}$;*ephrin-A5*$^{-/-}$ (knockout) mice. In wild-type mice, *lacZ*-positive axons form glomeruli almost exclusively in the anterior AOB (see also Belluscio et al., 1999), whereas in *ephrin-A5*$^{-/-}$ mice *lacZ*-positive axons project to the topographically inappropriate posterior AOB (indicated by black arrows, middle row) and to the anterior AOB (white arrows). In both cases, three adjacent (or almost adjacent) sections are shown, covering about 50 μm in depth of the medial AOB. More lateral sections are arranged to the left. (Bottom row) VN12-tau-*lacZ*$^{+}$;*ephrin-A5*$^{-/-}$ mice (showing topographic targeting errors in the AOB) were analysed for a proper development of the VNO by hybridising adjacent sections with $G_{\alpha i2}$- and $G_{\alpha o}$-specific probes. The staining pattern in these mice is in principle indistinguishable from the pattern obtained from VN12-tau-*lacZ*$^{+}$;*ephrin-A5*$^{+/+}$ mice, that is there is a good separation into basal and apical VNO as seen in the reciprocal expression of $G_{\alpha i2}$ and $G_{\alpha o}$.

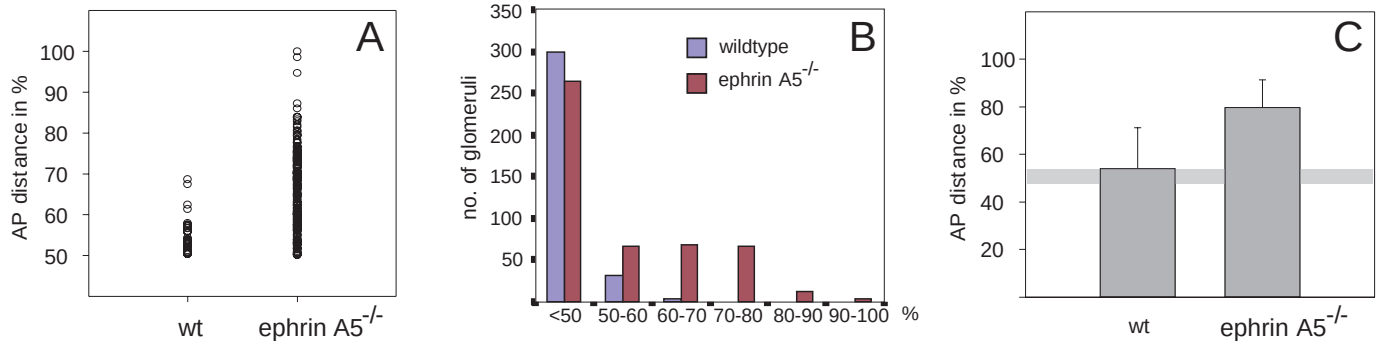

Fig. 7. Quantitative analysis of the location of VN12 receptor-expressing (*lacZ*-positive) glomeruli in wild-type and *ephrin-A5*$^{-/-}$ mice. In total, 14 wild-type and 14 *ephrin-A5*$^{-/-}$ mice were analysed. In each case a comparable number of adjacent sections from the medial part of the AOB were scored, typically about 10. Using the analySIS software, we measured first the total length of the AOB along the anteroposterior axis and then the location of each individual *lacZ*-positive glomerulus, taking the anterior pole as the reference point. (A) The location of individual VN12 positive glomeruli in wild-type and *ephrin-A5*$^{-/-}$ mice is indicated by single circles. Only data for the posterior AOB (50%-100%) are shown (with 0% at the anterior pole and 100% at the posterior pole). (B) Absolute numbers of VN12 positive glomeruli are plotted versus various parts of the posterior AOB. (C) By scoring the most posteriorly located glomerulus in each AOB, we found that – on average – in wild-type this is at a position about 54% from the anterior pole (indicating almost no overshooting into the posterior AOB), whereas, in *ephrin-A5*$^{-/-}$ mice, the most posteriorly located labelled glomerulus is found – on average –80% from the anterior pole (P=<0.001, t-test).

projection to the posterior AOB (data not shown). In contrast, in VN12-tau-*lacZ*$^{+}$;*ephrin-A5*$^{-/-}$ mice this typical projection pattern appeared disturbed in nine out of 14 cases analysed: β-galactosidase-positive axons projected to both the anterior and posterior halves of the AOB (Fig. 6, middle row; Fig. 8). Moreover, whereas in wild-type mice glomeruli were formed in both the medial and lateral part of the anterior AOB, we observed in *ephrin-A5*$^{-/-}$ mice a strong tendency of the misprojecting axons to form glomeruli in the medial third portion closest to the incoming vomeronasal nerve (not shown).

The number and position of stained glomeruli was measured in comparable medial sections in both wild-type and knockout mice (Fig. 7). Based on a neutral red staining, we first determined the length of the AOB with respect to the anteroposterior axis. The average size of the AOB in knockout and wild-type mice appeared rather similar (850 μm vs. 911 μm). Also, the number of β-galactosidase-positive glomeruli counted was comparable: in total about 300 β-galactosidase-positive glomeruli from wild-type mice and about 400 from knockout mice were counted.

A statistical analysis of these data revealed that in *ephrin-A5*$^{-/-}$ mice the overall position of β-galactosidase-positive glomeruli is shifted significantly toward the posterior pole as shown in Fig. 7, where the position of each individual labelled glomerulus located in the posterior part of the AOB is plotted. Fig. 7B shows absolute numbers of VN12 positive glomeruli in the posterior AOB of wild-type and mutant mice. When setting the anterior pole to 0% and the posterior pole to 100%, we found that the most posteriorly located glomerulus in each AOB of wild-type and *ephrin-A5*$^{-/-}$ mice is – on average –

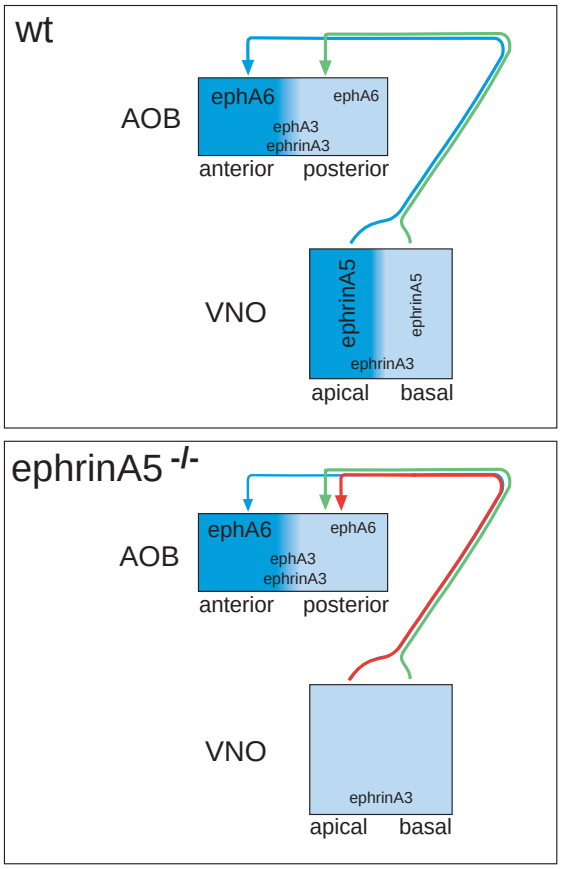

Fig. 8. The misprojection of vomeronasal axons in *ephrin-A5*$^{-/-}$ mice. (A) In wild type, ephrin-A3 is uniformly expressed in the VNO sensory epithelium and ephrin-A5 is expressed at a higher level in the apical than the basal VNO. No EphA receptors are expressed in this structure. In the AOB, ephrin-A3 (data not shown) and EphA3 are uniformly expressed, and EphA6 is expressed at a higher level in the anterior than in the posterior part of the AOB. The differential expression of EphA6 with respect to the mediolateral axis is not indicated here (medial>lateral). Axons from the apical VNO project to the anterior AOB and axons from the basal VNO to the posterior AOB. (B) In *ephrin-A5*$^{-/-}$ mice, axons from the apical VNO project to both the anterior and posterior AOB. On the basis of a statistical analysis of 14 *ephrin-A5*$^{-/-}$ mice, there is no apparent bias of apical VNO axons to project to either the anterior or posterior AOB (see Fig. 7).

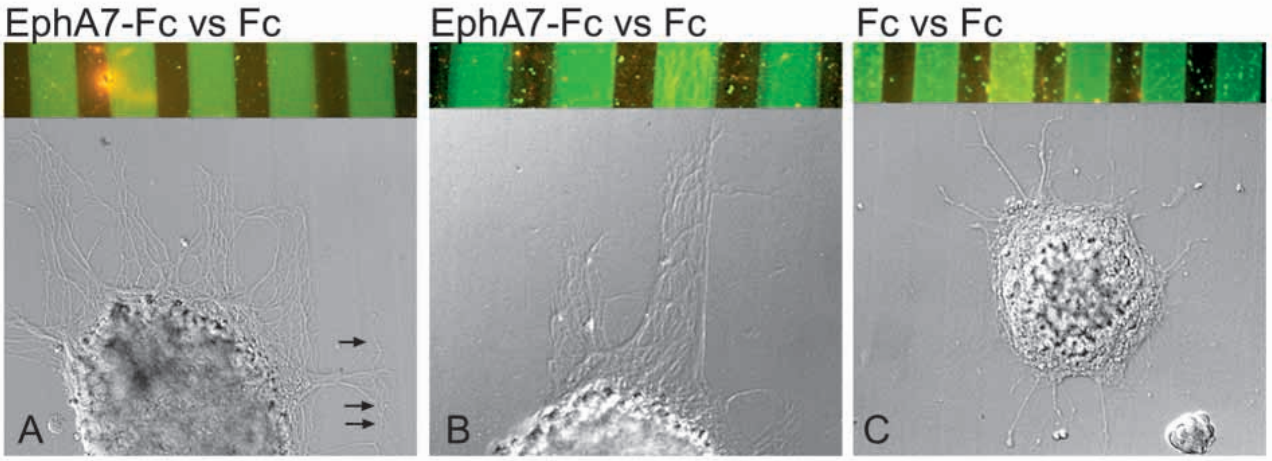

Fig. 9. Analysis of the growth behaviour of vomeronasal axons in the stripe assay. Carpets were prepared consisting of alternating stripes of EphA7-F_c versus F_c proteins – and as a control F_c versus F_c protein – which were subsequently treated with laminin. On these carpets, VNO explants of E14.5 mice were arranged. The cultures were incubated for 2 days, after which the outgrowth patterning was analysed. On F_c/F_c carpets, vomeronasal axons did not show a preference, and outgrowth of axons on these stripes was not very pronounced (C). On EphA-F_c/F_c carpets (A,B), a higher number of axons grew out, and showed a strong preference for EphA-F_c stripes. Stripes containing EphA-F_c have been labelled by addition of FITC-dextran (green). Arrows in A highlight an area where axons make sharp turns into an EphA-F_c stripe, after crossing an F_c stripe.

about 54% from the anterior pole in wild type and 80% away in knockouts (Fig. 7C).

No differences in lamination were observed in the VNOs and AOBs of wild-type and *ephrin-A5*$^{-/-}$ mice, suggesting that in mutant mice the development of these structures proceeds normally, at least from a gross morphological point of view. This finding was confirmed by an in situ hybridisation analysis using $G_{\alpha i2}$- and $G_{\alpha o}$-specific probes (Fig. 6, bottom row).

In the stripe assay, vomeronasal axons show a preference for growing on lanes containing EphA-F_c

The stripe assay, originally developed by Bonhoeffer and collegues (Walter et al., 1987), is a well suited in vitro assay system to study mechanisms and molecules involved in guiding axons. We have used this assay to establish an in vitro system for analysing the growth behaviour of ephrin-A-expressing vomeronasal axons in response to an EphA-containing substrate. For this, we used a modified stripe assay technique, in which soluble proteins can be arranged in alternating stripes on a nitrocellulose surface using a special silicone matrix (Hornberger et al., 1999; Vielmetter et al., 1990). We have prepared 'carpets' of alternating stripes, consisting of EphA7-F_c chimeric protein versus F_c protein, which were subsequently treated with laminin. The sensory epithelium of the vomeronasal organ from E14.5 mice was then isolated, chopped into small pieces and arranged onto the striped carpet.

2 days later, the axonal outgrowth pattern was analysed. We found that in controls (F_c versus F_c), vomeronasal axons showed no preference for either the first- or second-generated stripe, thus grew equally well on both stripes (Fig. 9C). The strength of outgrowth was similar to that found if vomeronasal axons are grown on a pure laminin substrate.

In stripe assays using EphA7-F_c versus F_c carpets, axons showed a clear preference towards growing on EphA-F_c-containing lanes (Fig. 9A,B). Occasionally, after crossing an F_c stripe and contacting an EphA-F_c-stripe, axons made a turn and spread into the EphA-F_c lanes (Fig. 9A, arrows). In general, the number of outgrowing axons was significantly increased when compared with the F_c/F_c substrate.

DISCUSSION

We have investigated the function of the EphA family during development of the mouse vomeronasal projection. Our studies have uncovered intriguing expression patterns of members of this family, in particular of ephrin-A5 with its differential expression in the VNO and of EphA6, with its graded expression in the accessory olfactory bulb, the target area of vomeronasal axons. These patterns indicate an important role for the EphA family in the formation of this projection, which is supported by results from both in vitro and in vivo experiments. In the stripe assay, vomeronasal axons show a preference for growing on lanes containing high EphA receptor concentrations, and in *ephrin-A5*$^{-/-}$ mice, the topographic targeting of vomeronasal axons in the accessory olfactory bulb is disturbed.

Ephrin-A ligand expression on vomeronasal axons

Looking at the subcellular protein distribution, it became clear that ephrin-A ligands are localised on VNO axons throughout the entire development of this projection, in contrast to EphA receptors, which could not be detected at either the mRNA or the protein level. An expression of ephrin-As on axons is not unusual in the EphA family and has already been reported, for example, in the main olfactory and the retinotectal systems. However, in those instances, both ephrin-A ligands and EphA receptors were shown to be expressed on olfactory axons (at least at some stages of development (St John et al., 2000; Zhang et al., 1996)) and on retinal ganglion cell axons (Hornberger et al., 1999).

The expression of ephrin-As on VNO axons suggests that

ephrin-A5 and ephrin-A3 exert in this context a 'receptor' function. Although this subclass of ephrins are bound to the membrane by a glycosylphosphatidylinositol (GPI) anchor, and thus on their own possess no direct link to the cytosolic compartment (Brown and London, 2000; Low, 1989), recent data have shown that ephrin-As have indeed the capacity for reverse signalling (i.e. into the ephrin expressing cell), possibly through engaging a transmembrane co-receptor. Here activation of ephrin-As by EphAs resulted in a β1-integrin-dependent increase in cell adhesion (Davy et al., 1999; Davy and Robbins, 2000; Huai and Drescher, 2001). Other examples of neuronally expressed GPI-anchored proteins capable of reverse signalling include contactin/F11 (Peles et al., 1997), Thy1 (Doherty et al., 1993), and the receptors for cilliary neurotrophic factor (Economides et al., 1995), glial-derived neurotrophic factor (Massague, 1996) and neurturin (Buj-Bello et al., 1997). Reverse signalling is also known to occur in the transmembrane ephrin-B ligands, and thus appears to be a characteristic of the entire Eph family (for review see Mellitzer et al., 2000).

The function of ephrin-As as receptors might be reflected by the seemingly complementary expression pattern of ephrin-As and EphAs in the target area of vomeronasal axons, the AOB, as revealed by AP-staining (Fig. 4). Here ephrin-A ligands localise to the dorsal AOB glomerular layer and EphA receptors to the mitral/tufted and granule cell layer. Close investigations of adjacent sections demonstrate a limited overlap in the expression of ligands and receptors in the glomeruli, i.e. at the interface between VNO axons and dendrites of mitral/tufted cells. As AP staining has to be interpreted with some caution (Sobieszczuk and Wilkinson, 1999), the precise extent of overlap of Eph and ephrin protein expression is difficult to judge using these probes, and it might require suitable antibodies.

However, the (mostly) reciprocal expression patterns of ephrin-As and EphAs within the AOB suggest a function of ephrin-As as receptors on invading vomeronasal axons and a function of EphAs as 'ligands' expressed on the dendrites of mitral/tufted cells in the glomerular layer. Such a concept is supported by the results from the stripe assay experiments (see below).

Vomeronasal versus retinotectal projection

It is generally thought that the formation of the retinotectal projection is controlled to a large extent by the reciprocal expression of members of the EphA family in projecting and target area such that retinal axons with a high EphA receptor concentration project to regions of the tectum with a low ligand concentration and vice versa (Drescher et al., 1997; Flanagan and Vanderhaeghen, 1998; O'Leary et al., 1999). The relationship between the respective ligand/receptor distribution and the axonal connection shown for the vomeronasal system is the opposite of that of the retinotectal system, as here a region with high ligand concentration, the apical VNO, is connected to a region of high receptor concentration, the anterior AOB. It is therefore possible that in the vomeronasal system, axonal projections are formed on the basis of interactions that are also opposite to the repulsive interactions seen for the retinotectal system, in other words, it would suggest an 'attractive' patterning principle in the AOB.

The behaviour of vomeronasal axons in the stripe assay

In support of such a concept, in the stripe assay vomeronasal axons prefer to grow on lanes containing EphA7-F_c/laminin, when offered the choice between EphA7-F_c/laminin- and F_c/laminin-containing lanes. On these EphA-F_c -lanes, axons grow out strongly and occupy the entire width of the stripes (Fig. 9A,B). Here, thick fascicles are often formed. On carpets consisting of F_c/laminin versus F_c/laminin stripes, no preference and weaker growth of vomeronasal axons was observed (Fig. 8C). The strength of growth on F_c/laminin was comparable with that on laminin alone, indicating no effect of F_c protein. Occasionally, we observed for EphA-F_c versus F_c and F_c versus F_c stripe assays (as well as explants on pure laminin) a ring of axons forming around (and in tight contact with) the explants, which indicates that vomeronasal neurones are capable of sending out axons under these conditions (Fig. 9C). Davy and Robbins reported a neurite outgrowth-promoting activity of EphAs for ephrin-A-expressing retinal axons (Davy and Robbins, 2000). This, however, is difficult to interpret as EphA molecules are also expressed on the axons (Hornberger et al., 1999).

The molecular mechanism of the preferential growth of vomeronasal axons on EphA-F_c lanes is presently not known and it is therefore not possible to give a precise description of this behaviour, which might be increased permissiveness, increased adhesion or even 'attraction'. However, a hint towards a mechanism involved is provided by recent findings that treatment of ephrin-A-expressing cells with EphA molecules results in a β1-integrin-dependent increase in adhesion of these cells, which depends on the activity of Src family kinases (Davy and Robbins, 2000; Huai and Drescher, 2001). Thus, a possible mechanism would be that activation of ephrin-As results – via an inside-out signalling mechanism – in an activation of integrins, which ultimately leads to the observed preference of vomeronasal axons for growing on EphA-F_c/laminin lanes. Such an idea would be consistent with an 'attractive' mechanism, because here a ligand-receptor system would actively regulate, via a signalling-dependent mechanism, axon-substrate interactions, in contrast to a 'permissiveness' that describes more passive axon-substrate properties.

In the context of the zonally organised vomeronasal projection, it is possible that ephrin-A-expressing vomeronasal axons are able to differentiate between different quantities and qualities of EphA receptor found in the anterior versus posterior AOB (Fig. 8).

The vomeronasal projection in *ephrin-A5*$^{-/-}$ mice

In *ephrin-A5*$^{-/-}$ mice the differential expression of ephrin-A molecules on vomeronasal axons is lost, resulting in the sole and uniform expression of ephrin-A3. This is likely to disturb the balance in the ephrin/Eph interaction and might be the cause of the phenotype observed in *ephrin-A5*$^{-/-}$ mice, i.e. the projection of apical VNO axons onto both the posterior and anterior AOB (Figs 6, 8). Indeed, this argues for a role of the higher expression of ephrin-A5 on apical VNO neurones in providing the corresponding ingrowing vomeronasal axons with the ability to discriminate between AOB regions with high and low levels of EphA6.

Overall, this system alone is unlikely to provide the

vomeronasal axons with the full guidance information (Gierer, 1998). In particular, one might predict the existence of additional components to antagonise these interactions – otherwise the entire population of VNO axons would grow into the (anterior) part of the AOB that has the highest receptor concentrations.

In the main olfactory system, many data indicate that the olfactory receptors themselves are crucially involved in the guidance of olfactory axons to their target areas. Thus, they might function as both odorant sensors and guidance receptors. A comparable role has been proposed for VNO receptors in the vomeronasal system. It will be of interest to analyse a possible interplay between the EphA family and vomeronasal receptors – for example, at the level of similar intracellular signalling pathways – and the contribution of each of these families to the guidance of vomeronasal axons.

We thank F. Bonhoeffer for discussions and support, C. Dulac for providing the VN12-tau-*lacZ* mouse line and advice in the analysis of these mice, and T. Ciossek for the F_c constructs. We also thank Alfred Gierer, Franco Weth, Michael Kiebler, Jürgen Löschinger and Rosemary Drescher for helpful comments on the manuscript. This work was supported by grants of the Deutsche Forschungsgemeinschaft to U. D. and by a European Union Biotechnology network grant to U. D.

REFERENCES

Bargmann, C. I. (1999). A complex sensory map for pheromones. *Neuron* **22**, 640-642.

Belluscio, L., Koentges, G., Axel, R. and Dulac, C. (1999). A map of pheromone receptor activation in the mammalian brain. *Cell* **97**, 209-220.

Berghard, A. and Buck, L. B. (1996). Sensory transduction in vomeronasal neurons: evidence for G alpha o, G alpha i2, and adenylyl cyclase II as major components of a pheromone signaling cascade. *J. Neurosci.* **16**, 909-918.

Berghard, A., Buck, L. B. and Liman, E. R. (1996). Evidence for distinct signaling mechanisms in two mammalian olfactory sense organs. *Proc. Natl. Acad. Sci. USA* **93**, 2365-2369.

Brown, D. A. and London, E. (2000). Structure and function of sphingolipid- and cholesterol-rich membrane rafts. *J. Biol. Chem.* **275**, 17221-17224.

Brückner, K., Pasquale, E. B. and Klein, R. (1997). Tyrosine phosphorylation of transmembrane ligands for Eph receptors. *Science* **275**, 1640-1643.

Brückner, K. and Klein, R. (1998). Signaling by Eph receptors and their ephrin ligands. *Curr. Opin. Neurobiol.* **8**, 375-382.

Buck, L. B. (2000). The molecular architecture of odor and pheromone sensing in mammals. *Cell* **100**, 611-618.

Buj-Bello, A., Adu, J., Pinon, L. G., Horton, A., Thompson, J., Rosenthal, A., Chinchetru, M., Buchman, V. L. and Davies, A. M. (1997). Neurturin responsiveness requires a GPI-linked receptor and the Ret receptor tyrosine kinase. *Nature* **387**, 721-724.

Callahan, C. A. and Thomas, J. B. (1994). Tau-beta-galactosidase, an axon-targeted fusion protein. *Proc. Natl. Acad. Sci. USA* **91**, 5972-5976.

Cheng, H. J. and Flanagan, J. G. (1994). Identification and cloning of ELF-1, a developmentally expressed ligand for the Mek4 and Sek receptor tyrosine kinases. *Cell* **79**, 157-168.

Ciossek, T., Monschau, B., Kremoser, C., Löschinger, J., Lang, S., Müller, B. K., Bonhoeffer, F. and Drescher, U. (1998). Eph receptor-ligand interactions are necessary for guidance of retinal ganglion cell axons in vitro. *Eur. J. Neurosci.* **10**, 1574-1580.

Daniel, T. O., Stein, E., Cerretti, D. P., St. John, P. L., Robert, B. L. and Abrahamson, D. R. (1996). ELF and LERK-2 in developing kidney and microvascular endothelial assembly. *Kidney Int.* **50**, S73-S81.

Davy, A., Gale, N. W., Murray, E. W., Klinghofer, R. A., Soriano, P., Feuerstein, C. and Robbins, S. M. (1999). Compartmentalized signaling by GPI-anchored ephrinA5 requires the fyn tyrosine kinase to regulate cellular adhesion. *Gen. Dev.* **13**, 3125-3135.

Davy, A., Feuerstein, C. and Robbins, S. M. (2000). Signaling within a caveolae-like membrane microdomain in human neuroblastoma cells in response to fibroblast growth factor. *J. Neurochem.* **74**, 676-683.

Davy, A. and Robbins, S. M. (2000). EphrinA5 modulates cell adhesion and morphology in an integrin-dependent manner. *EMBO J.* **19**, 5396-5405.

Doherty, P., Singh, A., Rimon, G., Bolsover, S. R. and Walsh, F. S. (1993). Thy-1 antibody triggered neurite outgrowth requires an influx of calcium into neurons via N- and L-type calcium channels. *J. Biol. Chem.* **122**, 181-189.

Drescher, U., Bonhoeffer, F. and Müller, B. K. (1997). The Eph family in retinal axon guidance. *Curr. Opin. Neurobiol.* **7**, 75-80.

Dulac, C. (2000). Sensory coding of pheromone signals in mammals. *Curr. Opin. Neurobiol.* **10**, 511-518.

Dulac, C. and Axel, R. (1995). A novel family of genes encoding putative pheromone receptors in mammals. *Cell* **83**, 195-206.

Economides, A. N., Ravetch, J. V., Yancopoulos, G. D. and Stahl, N. (1995). Designer cytokines: targeting actions to cells of choise. *Science* **270**, 1351-1353.

Flanagan, J. G. and Leder, P. (1990). The *kit* ligand: a cell surface molecule altered in steel mutant fibroblasts. *Cell* **63**, 185-194.

Flanagan, J. G. and Vanderhaeghen, P. (1998). The ephrins and Eph receptors in neural development. *Annu. Rev. Neurosci.* **21**, 309-345.

Frisen, J., Holmberg, J. and Barbacid, M. (1999). Ephrins and their Eph receptors: multitalented directors of embryonic development. *EMBO J.* **18**, 5159-65.

Gale, N. W., Holland, S. J., Valenzuela, D. M., Flenniken, A., Pan, L., Ryan, T. E., Henkemeyer, M., Strebhardt, K., Hirai, H., Wilkinson, D. G., Pawson, T. and Yancopoulos, G. D. (1996). Eph receptors and ligands comprise two major specificity subclasses and are reciprocally compartmentalized during embryogenesis. *Neuron* **17**, 9-19.

Gierer, A. (1998). Possible involvement of gradients in guidance of receptor cell axons towards their target position on the olfactory bulb. *Eur. J. Neurosci.* **10**, 388-391.

Grant, P., Tseng, D., Gould, R. M., Gainer, H. and Pant, H. C. (1995). Expression of neurofilament proteins during development of the nervous system in the squid Loligo pealei. *J. Comp. Neurol.* **356**, 311-326.

Halpern, M. (1987). The organization and function of the vomeronasal system. *Annu. Rev. Neurosci.* **10**, 325-362.

Henkemeyer, M., Orioli, D., Henderson, J. T., Saxton, T. M., Roder, J., Pawson, T. and Klein, R. (1996). Nuk controls pathfinding of commissural axons in the mammalian central nervous system. *Cell* **86**, 35-46.

Herrada, G. and Dulac, C. (1997). A novel family of putative pheromone receptors in mammals with a topographically organized and sexually dimorphic distribution. *Cell* **90**, 763-773.

Hinds, J. W. (1968). Autoradiographic study of histogenesis in the mouse olfactory bulb. I. Time of origin of neurons and neuroglia. *J. Comp. Neurol.* **134**, 287-304.

Holash, J. A., Soans, C., Chong, L. D., Shao, H., Dixit, V. M. and Pasquale, E. B. (1997). Reciprocal expression of the Eph receptor Cek5 and its ligand(s) in the early retina. *Dev. Biol.* **182**, 256-269.

Holder, N. and Klein, R. (1999). Eph receptors and ephrins: effectors of morphogenesis. *Development* **126**, 2033-2044.

Holland, S. J., Gale, N. W., Mbamalu, G., Yancopoulos, G. D., Henkemeyer, M. and Pawson, T. (1996). Bidirectional signalling through the eph-family receptor Nuk and its transmembrane ligands. *Nature* **383**, 722-725.

Holland, S. J., Peles, E., Pawson, T. and Schlessinger, J. (1998). Cell-contact-dependent signalling in axon growth and guidance: Eph receptor tyrosine kinases and receptor protein tyrosine phosphatase beta. *Curr. Opin. Neurobiol.* **8**, 117-127.

Holmberg, J., Clarke, D. L. and Frisen, J. (2000). Regulation of repulsion versus adhesion by different splice forms of an Eph receptor. *Nature* **408**, 203-206.

Hornberger, M. R., Dutting, D., Ciossek, T., Yamada, T., Handwerker, C., Lang, S., Weth, F., Huf, J., Wessel, R., Logan, C., Tanaka, H. and Drescher, U. (1999). Modulation of EphA receptor function by coexpressed ephrinA ligands on retinal ganglion cell axons. *Neuron* **22**, 731-742.

Horowitz, L. F., Montmayeur, J. P., Echelard, Y. and Buck, L. B. (1999). A genetic approach to trace neural circuits. *Proc. Natl. Acad. Sci. USA* **96**, 3194-3199.

Huai, J. and Drescher, U. (2001) An ephrinA-dependent signaling pathway controls integrin function and is linked to the tyrosine phosphorylation of a 120 kDa protein. *J. Biol. Chem.* (in press).

Huynh-Do, U., Stein, E., Lane, A. A., Liu, H., Ceretti, D. P. and Daniel, T. O. (1999). Surface densities of ephrin-B1 determine EphB1-coupled activation of cell attachment through avß3 and a5b1 integrins. *EMBO J.* **18**, 2165-2173.

Ichikawa, M., Takami, S., Osada, T. and Graziadei, P. (1994). Differential development of binding sites of two lectins in the vomeronasal axons of the rat accessory olfactoy bulb. *Dev. Brain Res.* **78**, 1-9.

Imamura, M., Mori, K., Fujita, S. and Obata, K. (1985). Immunocytochemical identification of subgroups of vomeronasal nerve fibers and their segregated terminations in the accessory olfactory bulb. *Brain Res.* **326**, 362-366.

Jia, C. and Halpern, M. (1996). Subclasses of vomeronasal receptor neurons: differential expression of G proteins (Gi alpha 2 and G(o alpha)) and segregated projections to the accessory olfactory bulb. *Brain Res.* **719**, 117-128.

Keverne, E. B. (1999). The vomeronasal organ. *Science* **286**, 716-720.

Krieger, J., Schmitt, A., Lobel, D., Gudermann, T., Schultz, G., Breer, H. and Boekhoff, I. (1999). Selective activation of G protein subtypes in the vomeronasal organ upon stimulation with urine-derived compounds. *J. Biol. Chem.* **274**, 4655-4662.

Low, M. G. (1989). The glycosyl-phosphatidylinositol anchor of membrane proteins. *Biochim. Biophys. Acta* 988, 427-454.

Massague, J. (1996). Crossing receptor boundaries. *Nature* **382**, 29-30.

Matsunami, H. and Buck, L. B. (1997). A multigene family encoding a diverse array of putative pheromone receptors in mammals. *Cell* **90**, 775-784.

Mellitzer, G., Xu, Q. and Wilkinson, D. G. (1999). Eph receptors and ephrins restrict cell intermingling and communication. *Nature* **400**, 77-81.

Mellitzer, G., Xu, Q. and Wilkinson, D. G. (2000). Control of cell behaviour by signalling through Eph receptors and ephrins. *Curr. Opin. Neurobiol.* **10**, 400-408.

Mombaerts, P., Wang, F., Dulac, C., Chao, S. K., Nemes, A., Mendelsohn, M., Edmondson, J. and Axel, R. (1996). Visualizing an olfactory sensory map. *Cell* **87**, 675-686.

Müller, B. K. (1999). Growth cone guidance: first steps towards a deeper understanding. *Annu. Rev. Neurosci.* **22**, 351-388.

O'Leary, D. D. M. and Wilkinson, D. G. (1999). Eph receptors and ephrins in neural development. *Curr. Opin. Neurobiol.* **9**, 65-73.

O'Leary, D. D. M., Yates, P. A. and McLaughlin, T. (1999). Molecular development of sensory maps: representing sights and smells in the brain. *Cell* **98**, 255-269.

Pandey, A., Shao, H. N., Marks, R. M., Polverini, P. J. and Dixit, V. M. (1995). Role of B61, the ligand for the eck receptor tyrosine kinase, in TNF-alpha-induced angiogenesis. *Science* **268**, 567-569.

Park, S., Frisen, J. and Barbacid, M. (1997). Aberrant axonal projections in mice lacking EphA8 (Eek) tyrosine kinase receptors. *EMBO J.* **16**, 3106-3114.

Peles, E., Nativ, M., Lustig, M., Grumet, M., Schilling, J., Martinez, R., Plowman, G. D. and Schlessinger, J. (1997). Identification of a novel contactin-associated transmembrane receptor with multiple domains implicated in protein-protein interactions. *EMBO J.* **16,** 978-988.

Rodriguez, I., Feinstein, P. and Mombaerts, P. (1999). Variable patterns of axonal projections of sensory neurons in the mouse vomeronasal system. *Cell* **97**, 199-208.

Ryba, N. J. and Tirindelli, R. (1997). A new multigene family of putative pheromone receptors. *Neuron* **19**, 371-379.

Schaeren-Wiemers, N. and Gerfin-Moser, A. (1993). A single protocol to detect transcripts of various types and expression levels in neural tissue and cultured cells: in situ hybridization using digoxigenin-labelled cRNA probes. *Histochemistry* **100**, 431-440.

Sobieszczuk, D. F. and Wilkinson, D. G. (1999). Masking of Eph receptors and ephrins. *Curr. Biol.* **9**, R469-R470.

St John, J. A., Tisay, K. T., Caras, I. W. and Key, B. (2000). Expression of EphA5 during development of the olfactory nerve pathway in rat. *J. Comp. Neurol.* **416**, 540-550.

Stein, E., Lane, A. A., Cerretti, D. P., Schoecklmann, H. O., Schroff, A. D., Van Etten, R. L. and Daniel, T. O. (1998). Eph receptors discriminate specific ligand oligomers to determine alternative signaling complexes, attachment, and assembly responses. *Genes Dev.* **12**, 667-678.

Tessier-Lavigne, M. and Goodman, C. S. (1996). The molecular biology of axon guidance. *Science* **274**, 1123-1133.

Vielmetter, J., Stolze, B., Bonhoeffer, F. and Stuermer, C. A. (1990). *In vitro* assay to test differential substrate affinities of growing axons and migratory cells. *Exp. Brain Res.* **81**, 283-287.

von Campenhausen, H. and Mori, K. (2000). Convergence of segregated pheromonal pathways from the accessory olfactory bulb to the cortex in the mouse. *Eur. J. Neurosci.* **12**, 33-46.

von Campenhausen, H., Yoshihara, Y. and Mori, K. (1997). O-CAM reveals segregated mitral/tufted cell pathways in developing accessory olfactory bulb. *NeuroReport* **8**, 2607-2612.

Walter, J., Kern-Veits, B., Huf, J., Stolze, B. and Bonhoeffer, F. (1987). Recognition of position-specific properties of tectal cell membranes by retinal axons *in vitro*. *Development* **101**, 685-696.

Wang, F., Nemes, A., Mendelsohn, M. and Axel, R. (1998). Odorant receptors govern the formation of a precise topographic map. *Cell* **93**, 47-60.

Wilkinson, D. G. (2000). Eph receptors and ephrins: regulators of guidance and assembly. *Int. Rev. Cytol.* **196**, 177-244.

Xu, Q., Mellitzer, G., Robinson, V. and Wilkinson, D. G. (1999). *In vivo* cell sorting in complementary segmental domains mediated by Eph receptors and ephrins. *Nature* **399**, 267-271.

Zhang, J.-H., Cerretti, D. P., Yu, T., Flanagan, J. G. and Zhou, R. (1996). Detection of ligands in regions anatomically connected to neurons expressing the Eph receptor Bsk: potential roles in neuron-target interaction. *J. Neurosci.* **16**, 7182-7192.

Zhou, R. P. (1998). The Eph family receptors and ligands. *Pharm. Ther.* **77**, 151-181.